DOI: 10.13009/EUCASS2022-7672

Experimental research on rocket re-usability by GNC parafoil

Authors : Ian Aenishanslin⋆, Julien Pain⋆⋆, Jean-Pierre Belmont⋆⋆⋆
Project members : Ian Aenishanslin⋆, Julien Pain⋆⋆, Pierre Loiseau⋆†, Remy Thuillier††
⋆*Ipsa Space Systems, IPSA*
63b Avenue Maurice Grandcoing, 94200 Ivry-sur-Seine, France
ian.aenishanslin@ipsa.fr · julien.pain@ipsa.fr

Abstract

This paper gives an overview of the project IPER (ISS Parafoil Experimental Rocket) from the student association Ipsa Space Systems that intends to develop and launch a rocket demonstrator to experiment the concept of recovery by GNC parafoil. The paper briefly discuss the design process of the demonstrator as well as the guidance strategy and simulations.

1. Introduction

After the recent success of rocket recovery and re-usability especially performed by SpaceX, the CNES (Centre National d'Etudes Spatiales) revived its studies on the domain. The French national space agency employs different means to enhance the research in the field of re-usability. In that context, the PERSEUS Project (Programme Europeen de Recherche Spatial Etudiant, Universitaire et Scientifique) is a CNES initiative educational project. The objective is to involve students on space programs and develop new technologies.
In this context, under the CNES request and consultation, the PERSEUS program has turned its roadmap towards the different technologies of re-usability such as thrust vectoring (the most known recovery means employed by SpaceX or under study on the french demonstrator Calisto), toss back or GNC (Guidance Navigation and Control) parafoil.

Our team being member of the student association Ipsa Space Systems part of the PERSEUS project since its beginning, decided to begin the very first study on GNC parafoil to recover a rocket stage 3 years ago when PERSEUS announced its roadmap. Since then, the IPER (ISS Parafoil Experimental Rocket) project is born with the objective to demonstrate a rocket recovery by self-guided (GNC) parafoil system.

The IPER rocket demonstrator already flew in 2021 after 2 years of development. The goal of this test flight was to test all the different subsystems without the GNC in order the validate the technical means. Now in 2022, the objective is to finally launch the rocket and recover it completely by GNC parafoil.

This report will therefore present the mechanical development and production of the demonstrator as well as the embedded systems development with all its software and GNC simulations.

2. Presentation, flight plan and preliminary design

2.1 Presentation

IPER is a 3 meters experimental rocket with diameter 160 mm. With a dry mass of 15 kg at launch, the apogee is expected to be around 1190 meters. This altitude gives enough time to control the parafoil and respects the rules imposed by the specifications.

The rocket is composed of three different parts coupled with three separation systems. Each part is equipped with a chute in order to recover the entire rocket in all flight scenarios. The main chute is a five meters wingspan parafoil controlled with actuators, the second parachute recovers the fairing part and the last one is used in case of emergency if anything goes wrong with previous ones. In a nominal flight scenario the parafoil will bring back the rocket body and

DOI: 10.13009/EUCASS2022-7672

all its subsystems to a location specified with coordinates. The fairing part will be recovered alone with its parachute.

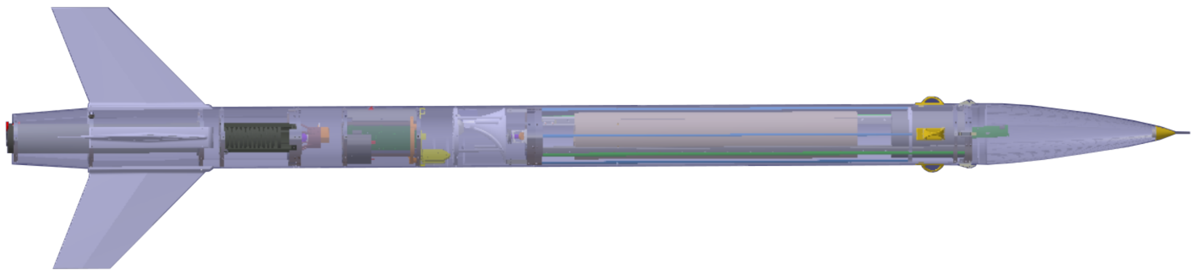

Figure 1: IPER global CAD view.

2.2 Flight plan

After 16 seconds of flight, IPER will reach the apogee of its trajectory and follow the nominal flight plan described hereafter.

- The first separation is activated and the fairing part is ejected (but still attached to the rocket) to deploy a drogue parachute. Then the rocket descends until an altitude of 500 meters under this drogue chute.
  Since exceeding 1500m of lateral shift is prohibited, considering the Lift to Drag ratio of the parafoil and the estimated average wind, 500 meters is the maximum altitude to begin parafoil operations.
- At 500 meters, the drogue chute as well as the fairing part are released from the rocket and extract the parafoil before leaving the rocket core and start their own descent.
- Parafoil operations begin : actuators control the parafoil and drive the rocket to the specified coordinates within the landing zone.

This is the flight plan if there are no failures. An emergency separation is nevertheless planned in case of problem. This separation splits the rocket in two parts and releases an third parachute. This system is called the Separation and Recovery System (SSR).

If the parafoil is in operation during the emergency separation, the new parachute will make the parafoil stall and so decrease the horizontal speed. This is the exact same process used by paraglider pilots during emergency where the secondary parachute is pulled to force the paraglide to stall.

Different emergency cases have been defined. If one of these cases is happening, the SSR will be released :

- A flight template has been defined, this is a 1.5 km circular pattern around the launch pad. An algorithm is constantly checking the rocket's position with real time GPS data. The rocket should not leave the flight template.
- The sink rate is also computed onboard to verify the proper descent in absence of stall or wrong deployment of one of the chute according to a certain threshold of 15m/s.

2.3 Aerodynamics Simulation

The preliminary design of the rocket is refined through computational fluid dynamics (CFD) simulation to help us adjust the trajectory in ascent phase. Indeed to actuation of the apogee separation system to deploy the first parachute is done by timing from the launch detection. Thus the characterization of the trajectory must be precisely done.
The simulation is a tunnel with an inlet of air at a speed of 160 m/s and an outlet at a pressure of 1 bar. The surface used for the simulation is the cross section of the rocket at ailerons level is $A = 0.029m^2$ and $\rho = 1.167kg/m^3$ the air density chosen at max Q corresponding altitude (around 500 m).

DOI: 10.13009/EUCASS2022-7672

Table 1: Computed parameters from CFD

	Computed value	Units
Drag force at max Q	82.4289	Newton
Drag coefficient	0.41	-

Running new trajectory simulations with these CFD parameters helped us obtain a better estimation of the apogee precise timing and corresponding height. This detail might be crucial since a wrong timing on the deployment can result in a destructive case on either, the chute surface or the rope attachment system itself due to important velocity at chute inflating.

In the results, the pressure and velocity of the air around the rocket help us understand better the aerodynamics of the rocket. The diameter's refinement at the rocket end might helps reduce the vortex at the end of the propulsive part. The stands of the rocket fins produce also a pressure loss, increasing the drag. Further Study would be useful to conclude on the efficiency of the diameter change to reduce the drag.

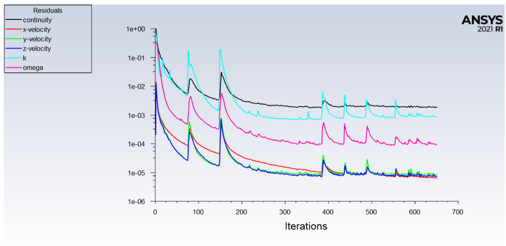

Figure 2: Residuals curve from CFD simulations. Continuity of 5×10^{-3} for 650 iterations.

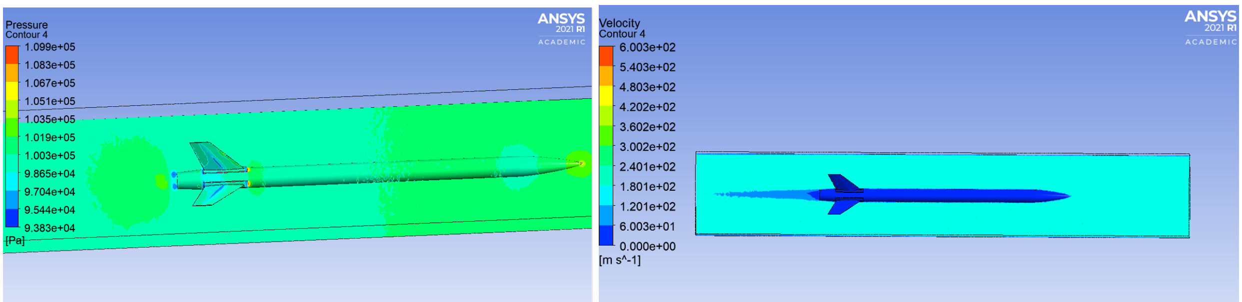

Figure 3: Pressure and Velocity simulations on IPER demonstrator.

3. Mechanical design

3.1 Experimental Part

The experimental part is the biggest part of the rocket, the tube is 1150 mm long. It includes the entire system of parafoil deployment, the drogue chute, rope management and the fairing separation system.

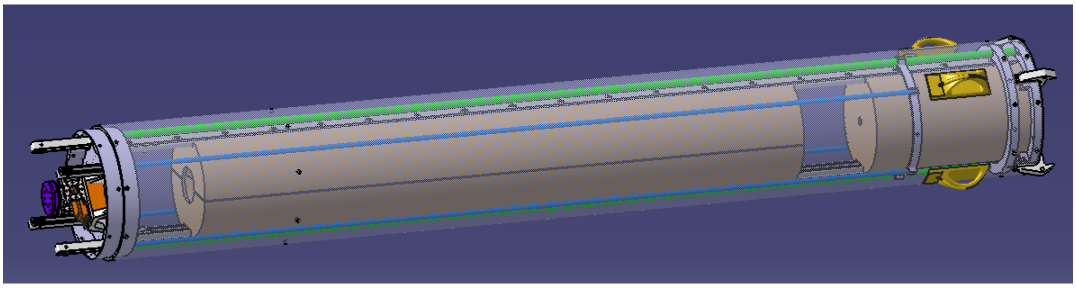

Figure 4: CAD representation of the experimental part containing the parafoil cases.

DOI: 10.13009/EUCASS2022-7672

3.2 Parafoil system

The goal of the parafoil system is the release of the parafoil at slow speed to be sure that the parafoil will not ripped and at desired height so that the rocket stay in the flight template. The parafoil is stored inside two half-shell of diameter 122 mm and the experimental part tube diameter is 152.8 mm inside. The ejection system is composed of 2 main cases, the parafoil case in two half-shell and the drogue chute case.

The drogue chute is above the parafoil case and he is ejected with the fairing at the apogee. Two rope passing in the green tubes link the latch and the drogue chute case. To avoid any unexpected ejection, the parafoil case is also link to the latch. At the desired height (500m) the latch unlocks the drogue chute and the parafoil case.

After the release, the drogue chute pulls the parafoil cases out. At the end of the drogue chute release, the drogue chute is link to the fairing and the parafoil cases disconnected from the rocket. The parafoil is linked to the rocket and deployed, ready to begin GNC operations.

The link between the rocket and the parafoil is composed of rope, slideway and rails. The rails are also use to guide the parafoil and drogue case during the exit of the rocket body. When the parafoil is ejected outside the rocket, the slideway will go to the top of the rocket.

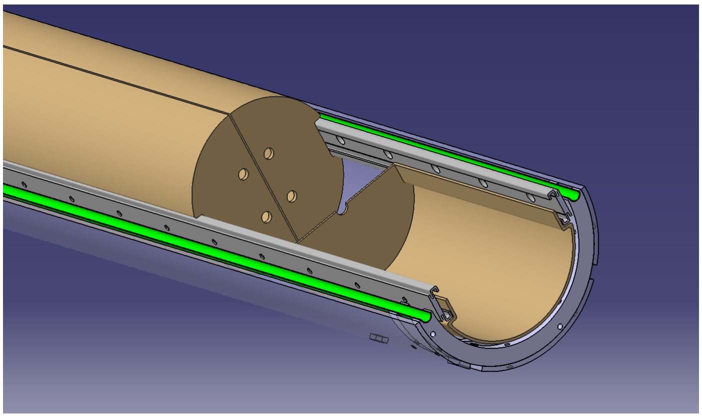

Figure 5: CAD Parafoil System

3.3 Control system of the parafoil

The control part is made of a 631.5 mm carbon fiber tube and contains two subsystems of the rocket. The first one is the control system of the parafoil that also holds the latch separation. The second one is the electronic bay, also called the on-board computer (OBC). The parafoil control system goal is the precise control of the parafoil brakes length.

The control of a parafoil uses two brakes, one on each side of the wing. The brakes act like ailerons but only go down when the rope is pulled. This phenomena creates drag on the pulled side. This make the wing turn towards this side.
The system is composed of two servomotors, one for each brake. The servomotor are able to make 4 turns to increase the usable length of the parafoil brakes. Each servomotor has a pulley (in violet on fig.[6])to increase the pulled length. The two servomotors are attached to the ring with a 3D printed part.

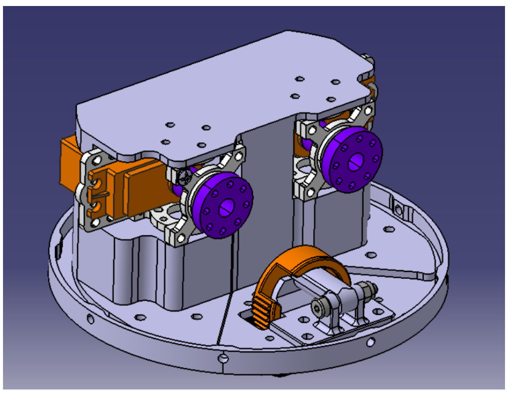

Figure 6: CAD of the control system.

DOI: 10.13009/EUCASS2022-7672

4. GNC parafoil development

The development of a GNC for a paragliding system has different challenges. The first point to be considered while elaborating a strategy is that without motorization system, we can consider the systems with a finite amount of energy, depending on how high the gliding phase starts. Thus, this energy must be managed and optimized as best as possible in order to match the objectives and reach the ground target as reliably as possible.

The second point, related to the first one, is the vulnerability of these kind of paragliding systems against the wind. Indeed, depending on the wing surface and loading, we can either choose a large wing surface, minimizing the wing loading and increasing the lift to drag ratio or choosing a high wing loading. With a small wing loading, the systems will be capable of greater gliding capabilities offering better maneuverability and flexibility to adjust its flight and reach the ground target. The drawback of this design choice will be the low forward gliding airspeed (around 7.5 m/s in our demonstrator) compared to the average wind speed those kind of systems can encounter in the atmosphere. Therefore, in certain cases, the high wing loading strategy (smaller wing surface) might be more suitable. For the IPER demonstrator we however went for a relatively low wing loading of $\approx 3kg/m^2$ (common in paragliding systems between $3kg/m^2$ and $5kg/m^2$) to maximize the gliding time since the objective is to study the gliding strategy and the starting height of the vehicle is relatively low (500m).

Thus, this compromise between gliding performance and wind robustness is to be considered and will be directly correlated to the GNC performance and reliability.

4.1 Guidance strategy

In this section we will exposed the guidance strategy used on IPER demonstrator, that consider these challenges and presents a promising wind robustness.

The objective of the strategy is to bring back the gliding vehicle to a landing point. In addition, a secondary objective is to land facing the wind to minimize the approach ground speed.
The GNC strategy will be exposed as below and illustrated with graphics resulting from our simulations to help visualize the concept.

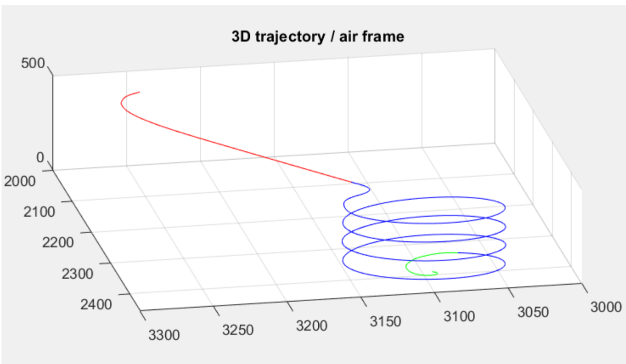

Figure 7: GNC strategy with 0 wind speed and *straight in* capture method.

Basic strategy

If we disregard the wind effect, the basic idea is to manage the relationship energy/range-to-go by varying the length of the ground track. For that, we have to define a nominal pattern, the ground track of which will be simply a circle centered on the target. Thus, the 3-D definition of this pattern is a cylinder called EMC (Energy Management Cylinder), the energy management consisting of varying the diameter of this cylinder as a function of the actual energy (i.e. the vehicle altitude).

DOI: 10.13009/EUCASS2022-7672

Considering the low airspeed of the vehicle with respect to the possible windspeed, the EMC cannot be a fixed pattern in ground axes, so it will be defined in a referential moving with the wind. Thus, it is necessary to have a certain knowledge of the wind profile prior to the flight. The trajectory of the EMC center can be seen as a particle falling in the air with the same vertical speed as the vehicle. This trajectory will be computed such as its final position (vehicle altitude = 0) coincides with the target location.

The strategy is decomposed in 3 phases :

- The Homing phase : The approach from the starting point, once the parafoil deployed after the rocket flight, in order to get closer to the targeted EMC. (red on fig. [7])
- The EMC phase : Once the vehicle sufficiently close to the EMC (condition on the distance between the vehicle and the EMC center), it switches into "Energy management mode" and descends in spiral around the EMC toward the ground. (blue on fig. [7])

  - The EMC capture refers to the transition phase where the algorithm decide to switch from the approach phase to the spiral phase. It can be done in different way. The "straight in" method capture the spiral once sufficiently close (solution chosen here, as in fig.[7]). The "overhead" method goes through the spiral, passes the spiral center overhead and catches the spiral from behind. This strategy allow to smoother the catch phase and reduce the trajectory oscillation that can appear during this phase.
- The Final phase : Once close to the ground (condition on the height of the vehicle), the vehicle switches into final mode where the vehicle quit the EMC by heading towards its center facing the wind. (green on fig. [7])

Air frame

However, to apply this strategy, the GNC has to clearly define the reference air frame which moves with the wind profile entered into the GNC prior to the flight. Thus its movement from a control point of view will be done in the air frame. This reference frame, denoted R_{air} moves following the wind with its direction Ψ and intensity WS during a period ΔT. Thus the air-frame's movement in the ground frame follows :

$$R_{air} = \begin{cases} WS.\Delta T.cos(\Psi) \\ WS.\Delta T.sin(\Psi) \end{cases} \quad ; \quad X_{air} = X_{ground} + R_{air} \tag{1}$$

When the wind speed is null, air frame is fixed relative to the ground frame and so, the GNC guidance follows the ideal case as in figure [7].
With a non-null wind (2m/s in this simulation), the strategy results in a shifting spiral as below :

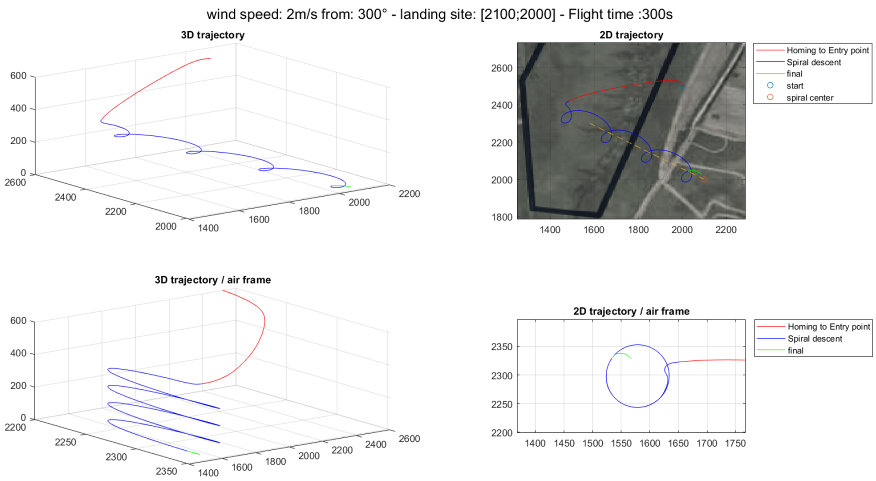

Figure 8: Simulation Results with 2m/s of windspeed.

DOI: 10.13009/EUCASS2022-7672

As we can see on the two bottom graph corresponding to the air frame, the spiral is circular as before because the control is relative to the air volume. In the two top graph corresponding to the ground frame however, the vehicle maintains its spiral but with a center sliding or shifting according to the wind.

Additionally, the Air-frame is defined precisely in the ground frame to match the position of the spiral center with the landing point when the height becomes null. Thus, the autopilot maintains the spiral in the airframe, regardless the landing point, and naturally ends over the landing site once close to the ground.
This is done by choosing a ΔT in the frame definition such that :

$$\Delta T = T_{gliding} - time = \frac{H_0}{V_z} - time \tag{2}$$

With H_0 being the height at the beginning of the GNC phase and V_z the constant vertical speed discussed.

Moreover, we also perform a rotation of the air frame in the ground frame around the z axis in order to be aligned with the wind direction. This operation will simplify the computation of the GNC once in EMC phase.

4.1.1 Energy management and landing

We thus take advantage of the EMC to adjust the trajectory and prepare the landing to exit at the correct position in order to land facing the wind.

To do so, we modulate the spiral radius in order to exit the EMC at an angle determined to travel, between the end of the spiral and the center of the spiral being the landing point, facing the wind. On figure [9], the goal is to exit the spiral at exit point to make the final landing towards the spiral's center facing the wind.

During the homing phase, we start preparing our EMC phase by predicting the interception/capture point with the EMC. With the altitude of this capture point, we can already compute a distance to be travelled during the EMC phase with a nominal spiral radius defined as initial condition. This remaining gliding distance can be associated with an unbounded angle θ_∞ defined as follow :

$$\Delta T = \frac{H}{V_z} = \frac{R(\theta_\infty + 1)}{V_h} \Rightarrow \theta_\infty = \frac{H}{R}\frac{V_h}{V_z} - 1 \tag{3}$$

By dividing this remaining travel angle θ_∞ by 2π and rounding the result to the lower integer, we define $k = \theta_\infty/2\pi$ as the number of spire to travel during the EMC at a nominal radius (taken at 50m in the simulations).

Once the EMC captured, we know the actual angular position of the vehicle θ in the spiral and the updated θ_∞ by adding up the $2k\pi$ decremented at each 2π during the descent.

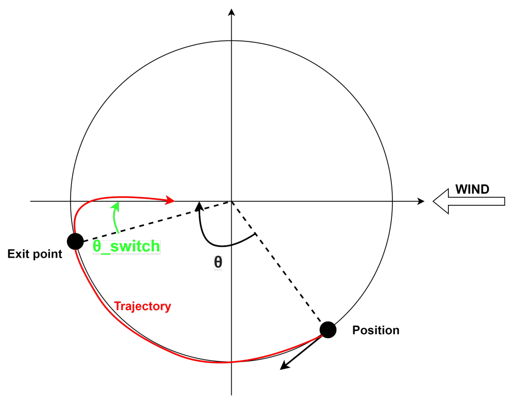

Figure 9: Spiral schematizing.

Thus, by measuring the altitude at each timestep and deducing the θ_∞, we can adjust the radius of the EMC from equation (3) as follow :

$$R = \frac{H}{(\theta_\infty + 1)}\frac{V_h}{V_z} \tag{4}$$

Additionally, we can switch into final mode toward the landing at a certain angle θ_{switch} before $\theta = 0$ in order to reduce the overshoot as schematized on fig. [9].

By modifying the radius as exposed above during the EMC phase, we modulate our cylinder and ensure that when we must exit the spiral, we should be at the correct exit point to perform our final phase facing the wind, thus minimizing our approach ground speed.

DOI: 10.13009/EUCASS2022-7672

4.2 Experimental approach of systems modelling

From the beginning of the project, the objective to demonstrate the technical feasibility of rocket stage recovery by GNC parafoil. The mathematical modelling of the paragliding systems requires a certain time and means such as wind tunnel to study the wing itself. In our case, with short deadlines and absence of aerodynamic data on the parafoil from the manufacturer, we opted an experimental approach.

Prototype test flights and data analysis

The approach for the study has been to constitute a flying prototype of the IPER demonstrator replicating its inertia (mass and their placement ; the inertia and gravity center position play an important role in the controlability and behavior) and perform a series of short flights applying step input in order to identify the response of the whole system in flight.

Figure 10: Photography of the prototype test flights.

Onboard, the flight is recorded with different sensors (GPS, IMU/AHRS, absolute pressure sensor) in order to identify the systems.

First, with the GPS ground trajectory and the height deduced form the pressure sensors with the standard atmospheric model, we could identify and average through the different flights aerodynamic constants :

Table 2: Averaged aerodynamic gliding parameters

	Average Value	Units
Sink rate	-2.5	m/s
Forward speed	7.5	m/s
L/D ratio	3	-

Those parameters have to be well estimated since the GNC algorithm will only rely on it in order to estimate its remaining energy, equivalent gliding time/distance.

This lift to drag ratio offers us a considerable gliding time but also, a important vulnerability to wind with its forward airspeed of only 7.5m/s.

DOI: 10.13009/EUCASS2022-7672

For the modelling of the behavior in response to our radio-commands, with the lack of quality on the GPS data, we decided to base our identification on the inertial data from the IMU.

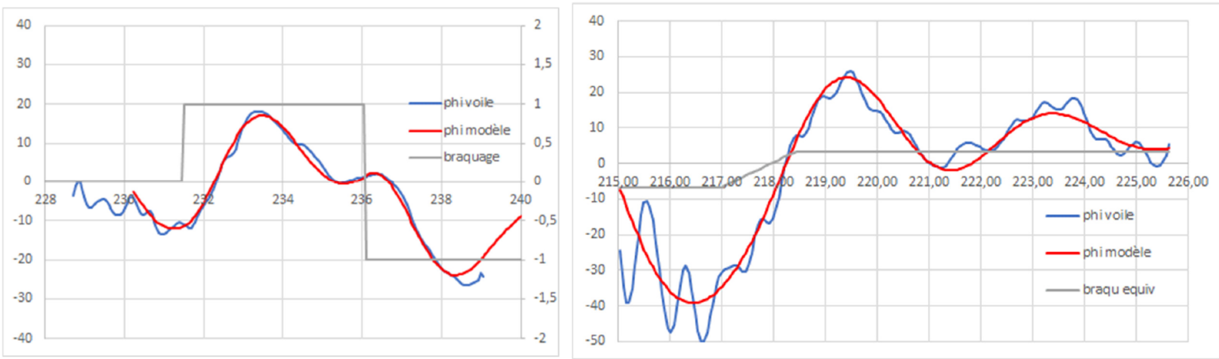

Figure 11: Model fitting on prototype two different test flight data. In blue the measured data (roll), in grey the step input applied, in red the model fitted.

On the above figure [11] we can see the model fitting around the measured data from different test flights done on the prototype. By observation of the oscillating behavior of the system in response to the step input through the different test flights, we estimated that a second order model would be sufficient in order to represent the response with the precision and requirement we have.

Thus the corresponding model is deduced :

$$\frac{\phi}{\mathbf{U}} = \frac{\mathbf{2.5}}{\mathbf{p^2 + 0.25p + 2.5}} \times \mathbf{2.5^\circ/cm} \tag{5}$$

With ϕ the roll angle and U the input being the braking command expressed in centimeters here the the static gain.

Another interesting result validated from those test flights is the characterisation of the oscillations in the payload under the parafoil. Indeed, beside the oscillation modeled above on the lateral and longitudinal behavior resulting form the control inputs, the payload has a constant oscillation around the vertical/rocket axis (z axis in yellow on fig. [12]). The fact this oscillation has an approximate frequency of $1.5Hz$ and an amplitude that can easily reach $100^\circ/s$ strengthens us in the idea that the control feedback can not directly be done based of the inertial measurement but on the GPS derivation instead.

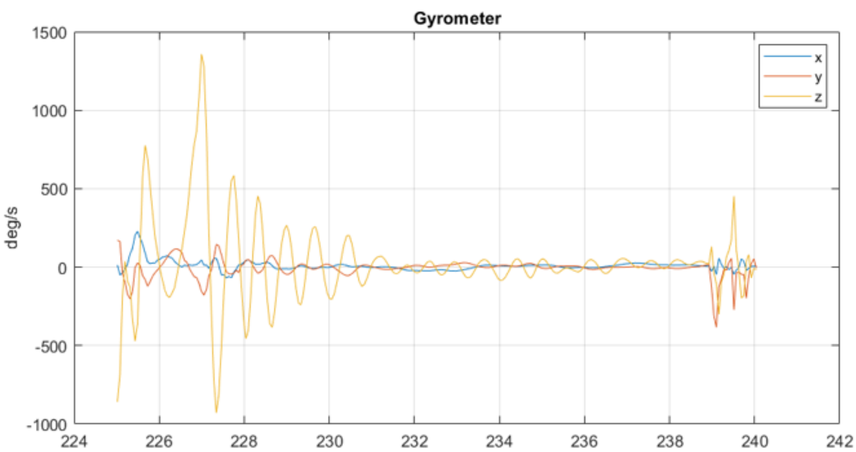

Figure 12: Gyrometer data (degree/second) from prototype test flight. In Yellow the oscillation visible around the z axis of the payload.

DOI: 10.13009/EUCASS2022-7672

4.3 Matlab/Simulink control simulation

To study the control theory of the GNC, a simulator has been developed on Matlab/Simulink. This ground software simulates the dynamics of the system identified and discussed in the previous sections and allows to develop the control algorithm that will be implemented in the flight OBC.

The idea is to build the simulator as modular as possible with every parameters tunable to study the most cases possible. Moreover, the Simulink has been anticipated and developed well before the model identification with a guessed dynamics. Thus, it has been done knowing that every parameter will change in the future.
Here is an overview of the Simulink :

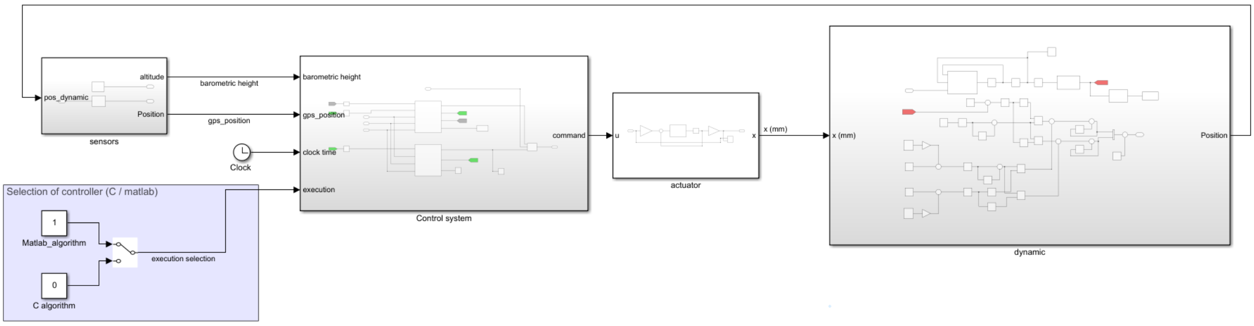

Figure 13: Simulink overview

This modular simulation tool allowed us to better understand the challenges of the GNC, especially concerning the wind. We could run simulation with wind speed comparable in magnitude with the forward gliding airspeed of the vehicle to test the robustness of the guidance strategy. On the bellow simulation (fig. [14]) with a $6m/s$ wind speed from heading 270°, we can see that, despite the trajectory appearance from the ground point of view not looking like a spiral anymore, the algorithm adapt and still manages to reach the ground target.

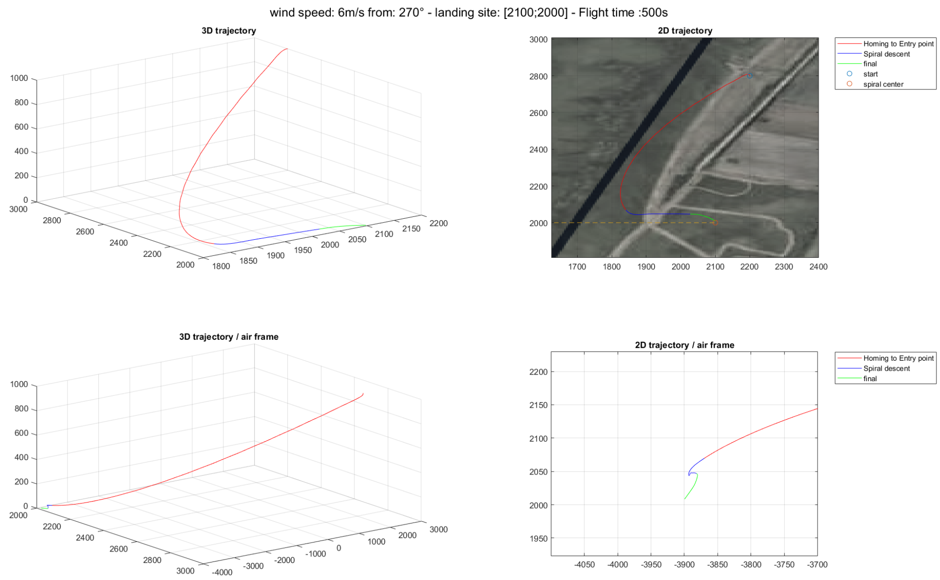

Figure 14: 6m/s wind speed simulation

The initial approach phase to capture is very long for two main reason. As the wind speed is large, for the center spiral to finish its course with the air mass above the landing site, it has to start farther. In addition the initial phase mostly always consists of flying upwind in order to catch the incoming spiral upstream. This is a convenient aspect of the strategy since it avoids the vehicle to be carried away by the wind downstream behind the landing site and not being able to navigate facing the wind back to the landing site before the touchdown.

DOI: 10.13009/EUCASS2022-7672

Thus, with the initial phase temporizing the flight, the vehicle spend a little time into the actual spiral and don't have the time to perform here a single spiral revolution. However, despite these unfavorable wind condition, the simulation shows that the guidance algorithm can find solutions in order to still match its objectives.

5. Conclusion

The IPER demonstrator is an ongoing project. It has already flew in 2021 without GNC algorithm in order to validate subsystems. After correction and improvement on the rocket platform concerning the parafoil deployment as well as finalization of the GNC algorithm and system modelling, the project will now be ready to perform its first complete test flight during the C'Space launch campain in 2022. Nevertheless, this project allowed our team and the PERSEUS project to deepen the reflection on GNC parafoil in general but also their integration and benefit in a rocket demonstrator. Although the design might be un-optimized since the parafoil in the IPER demonstrator occupies the entire payload segment of the rocket due to the small diameter of the demonstrator. However this recovery technology might appears very efficient and economic on larger rocket stage.

6. Acknowledgment

Thanks to Renaud Vallette, member of Ipsa Space Systems who participated in some designs of the project and also in the mechanical production.

Thanks to CNES with the PERSEUS project for allowing us to take part in these development and accompanying us through this project.

Thanks to M. Belmont who previously worked on GNC parafoil and agreed to share with us his wide expertise about the subject. The theoretical development of the GNC would not have been such complete, interesting and enriching without his precious help.

Finally, we also want to thank our school IPSA and our sponsors (Turgis & Gaillard, CNES, Thales, ADDL) for allowing us financially to achieve this project.